

Supplementary Figures

Tumor-associated Reactive Astrocytes Aid the Evolution of Immunosuppressive Environment in Glioblastoma

Dieter Henrik Heiland^{1,3,11,#}, Vidhya M. Ravi^{2,3,11,#}, Simon P. Behringer^{1,3,11}, Jan Hendrik Frenking^{1,3,11}, Julian Wurm^{1,3,11}, Kevin Joseph^{2,3,11}, Nicklas W.C. Garrelfs^{1,3,11}, Jakob Strähle^{3,11}, Sabrina Heynckes^{1,3,11}, Jürgen Grauvogel^{3,11}, Pamela Franco^{3,11}, Irina Mader^{4,5}, Matthias Schneider⁶, Anna-Laura Potthoff⁶, Daniel Delev⁷, Ulrich G. Hofmann^{2,3,11}, Christian Fung^{3,11}, Jürgen Beck^{3,11}, Roman Sankowski^{8,11}, Marco Prinz^{8,9,10,11}, Oliver Schnell^{1,3,11}

¹*Translational NeuroOncology Research Group, Medical Center, University of Freiburg, Germany*

²*Neuroelectronic Systems, Medical Center, University of Freiburg, Germany*

³*Department of Neurosurgery, Medical Center, University of Freiburg, Germany*

⁴*Department of Neuroradiology, Medical Center - University of Freiburg, Germany*

⁵*Clinic for Neuropediatrics and Neurorehabilitation, Epilepsy Center for Children and Adolescents, Schön Klinik, Vogtareuth, Germany*

⁶*Department of Neurosurgery, University of Bonn, Bonn, Germany*

⁷*Department of Neurosurgery, University of Aachen, Aachen, Germany*

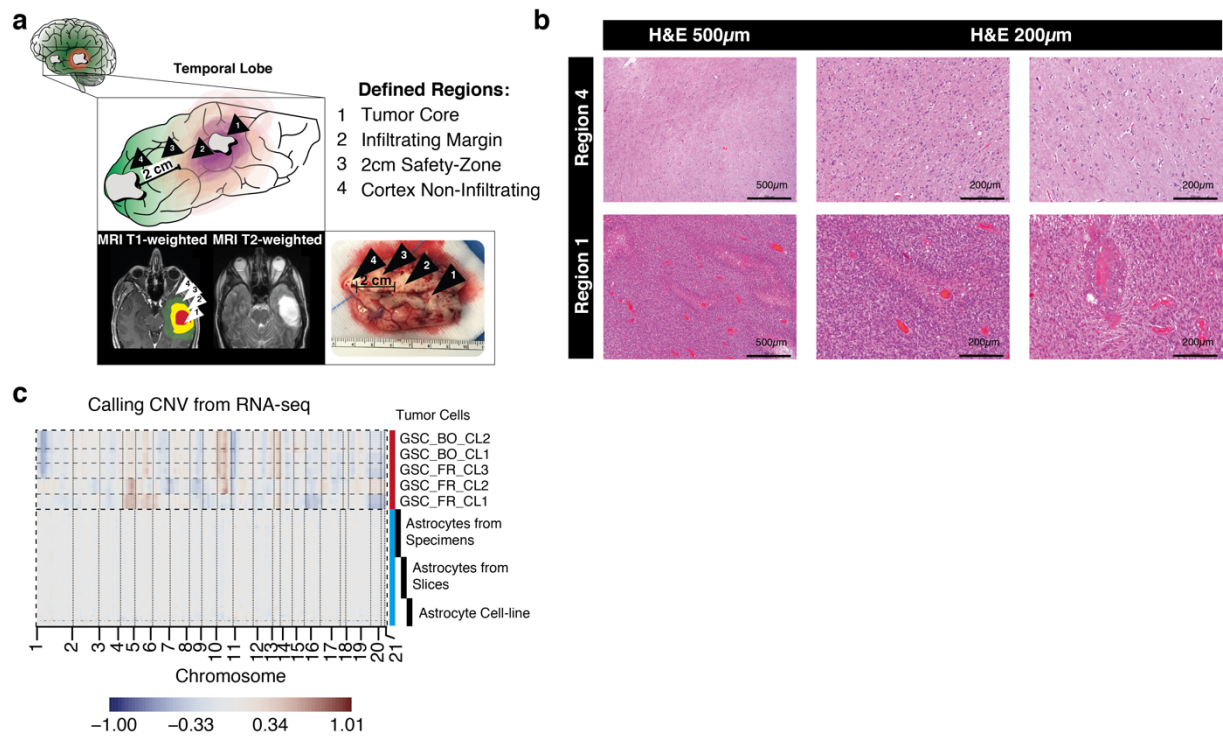
⁸*Institute of Neuropathology, Medical Center - University of Freiburg,*

⁹*Signalling Research Centres BIOSS and CIBSS, University of Freiburg, Germany*

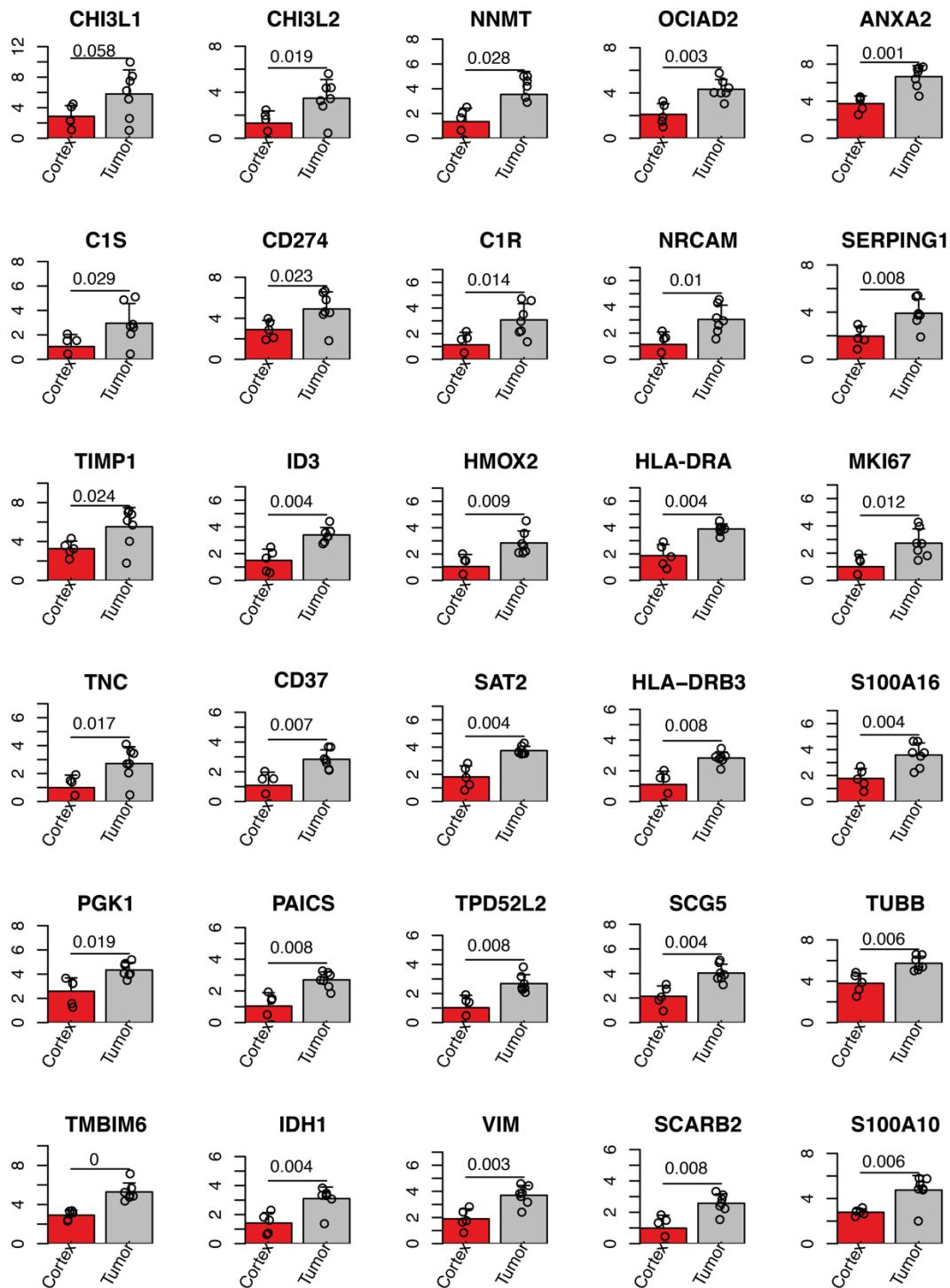
¹⁰*Center for NeuroModulation (NeuroModul), University of Freiburg, Freiburg, Germany.*

¹¹*Faculty of Medicine, Freiburg University, Germany*

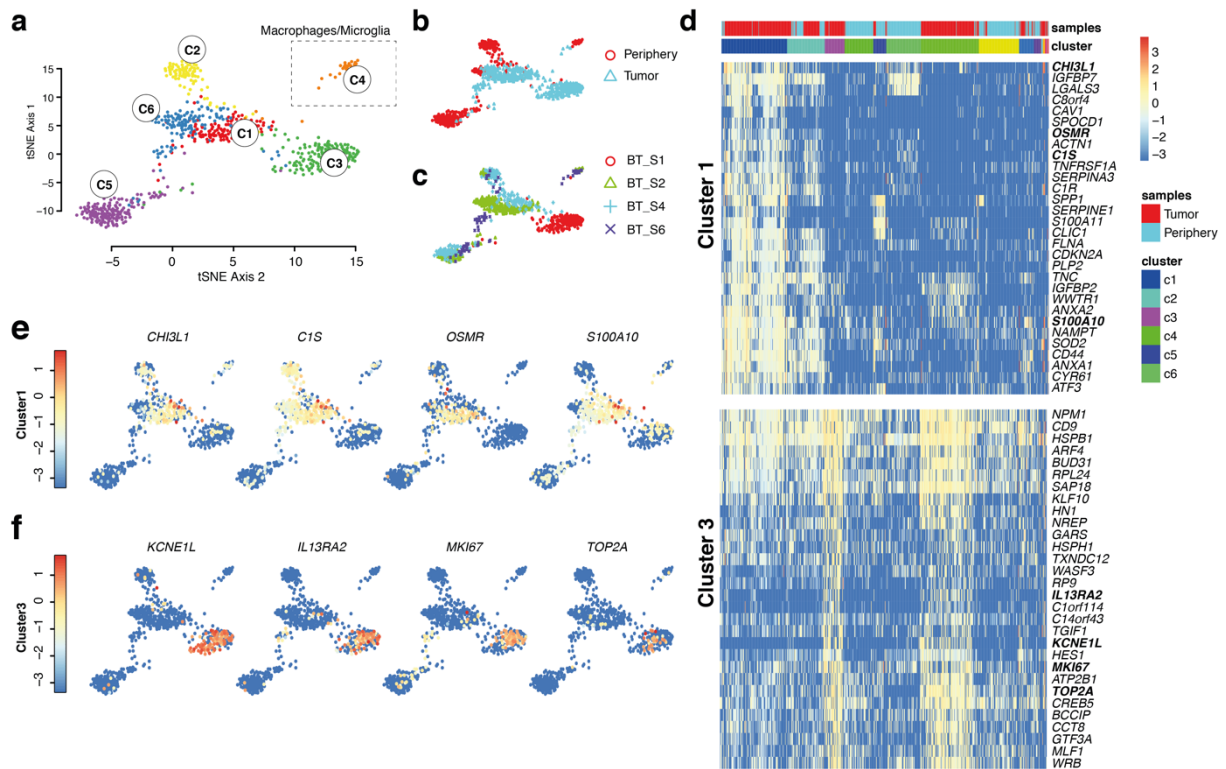
These authors contributed equally



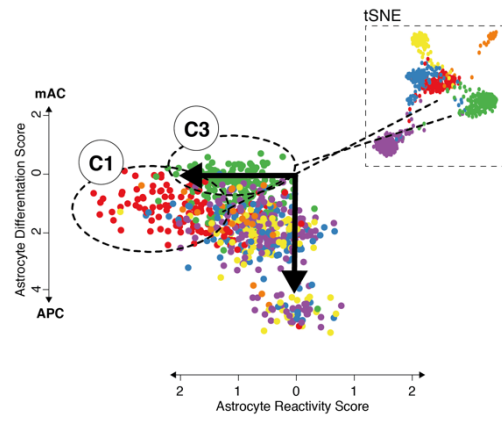
Supplementary Figure1: **a)** The figure illustrates the preoperative planning to identify the localization for intraoperative sampling. In order to avoid tumor contamination of the “cortex non-infiltrating” region we ensure a minimum distance to MRI signal alteration of at least 2cm (left bottom panel). The tumor was resected on-block and preoperatively planned regions were marked by neuronavigation, controlled in the resected specimen, sampling of the determined regions was done ex-vivo (right bottom panel). To prevent tissue degradation, we performed all sampling steps in the Operation Theater directly. **b)** Representative H&E stainings from region 1 and 4 are illustrated. **c)** In order to validate the tumor cell contamination, we call copy-number-variance of all purified astrocytes and tumor cell lines for control.



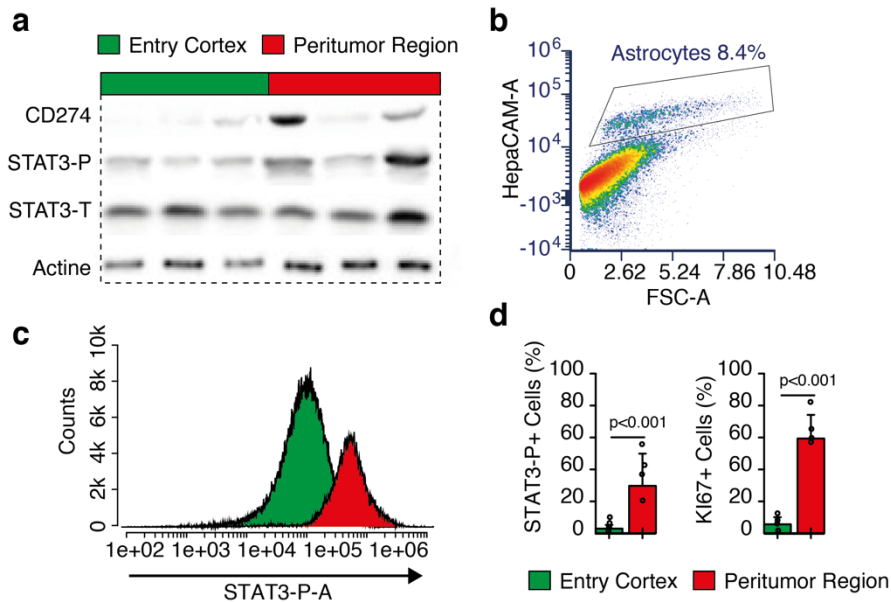
Supplementary Figure2: Bar plots of 30 most up-regulated genes in tumor associated astrocytes vs. astrocytes from non-malignant tissue. Expression values of the x-axis are normalized log2 transformed count data. P-values were determined by two-tailed Student's t-test adjusted by Benjamini-Hochberger for multiple testing. Data is given as mean \pm standard deviation.



Supplementary Figure 3: a) Analysis of single-cell RNA sequencing Data from Darmanis and colleagues. TSNE map of RaceID clustering revealed 5 astrocyte cluster (C4 contained dominantly myeloid cells). With distinct transcriptional differences between tumor and infiltrating regions b). Clustering of most differently expressed genes of the tumor associated genes was illustrated in d) and in colored TSNE maps in e).

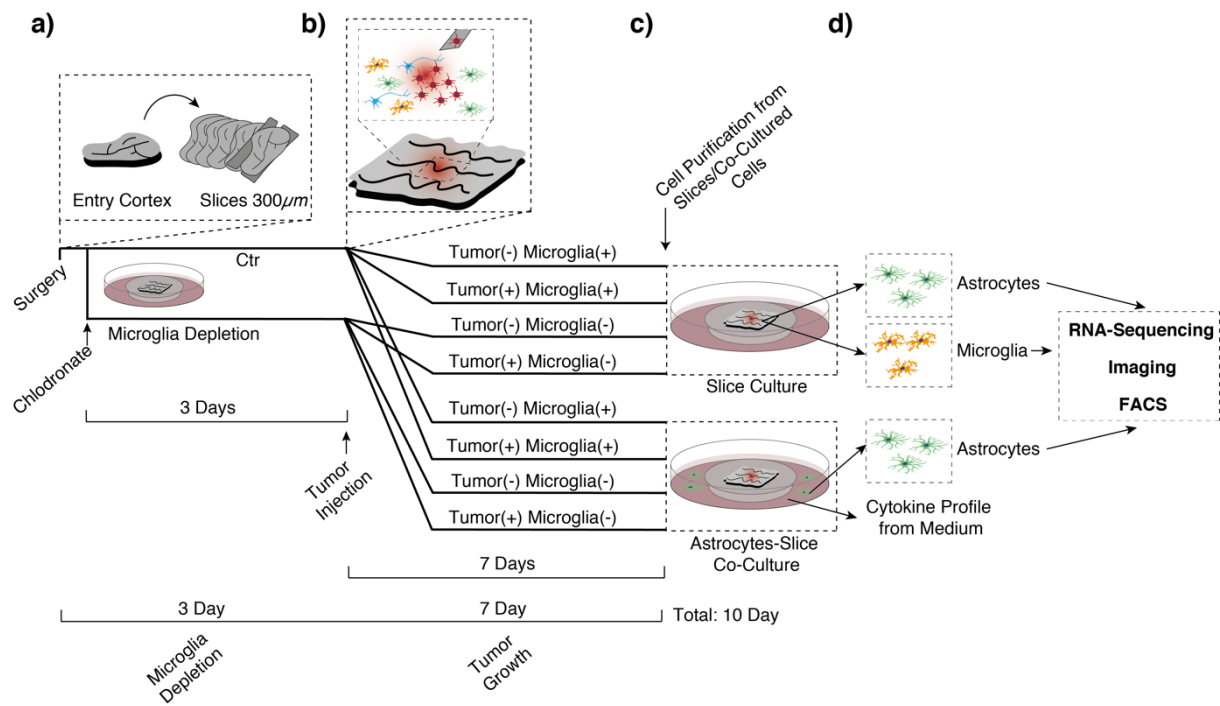


Supplementary Figure4: Two-dimensional scatterplot of astrocytic differentiation and reactivity as shown in Figure 1, from single-cell RNA sequencing Data from Darmanis and colleagues

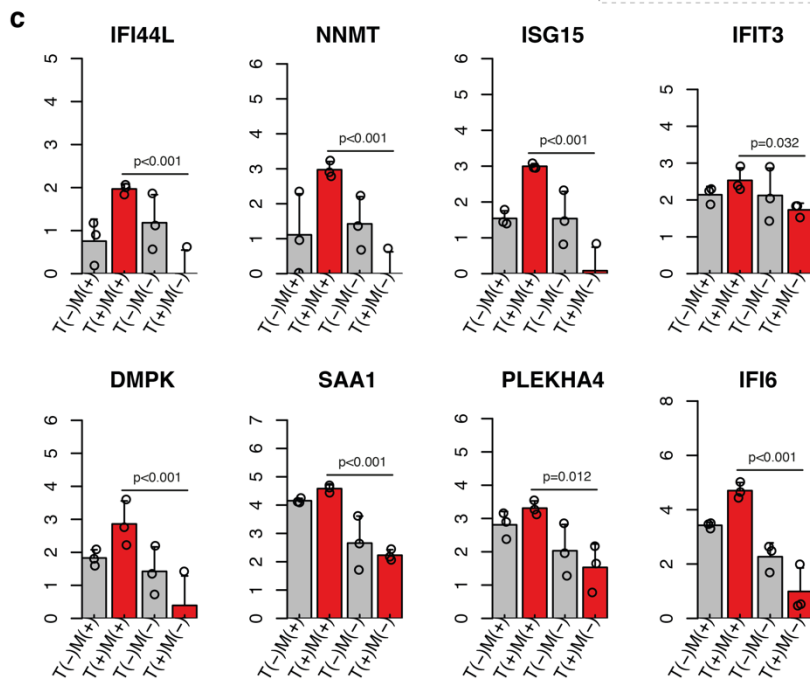
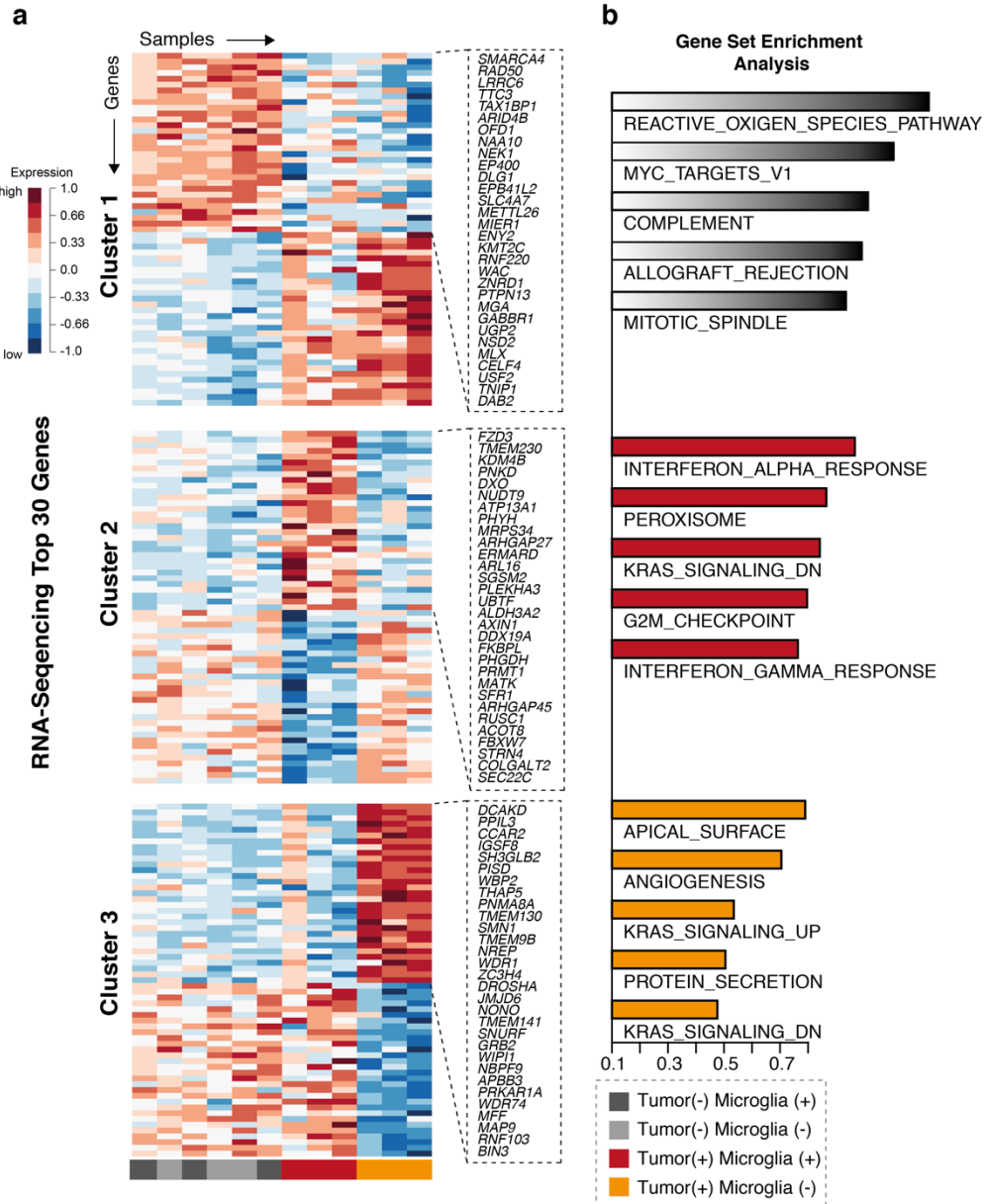


Supplementary Figure 5: Workflow und sample collection and Tumor-injection model

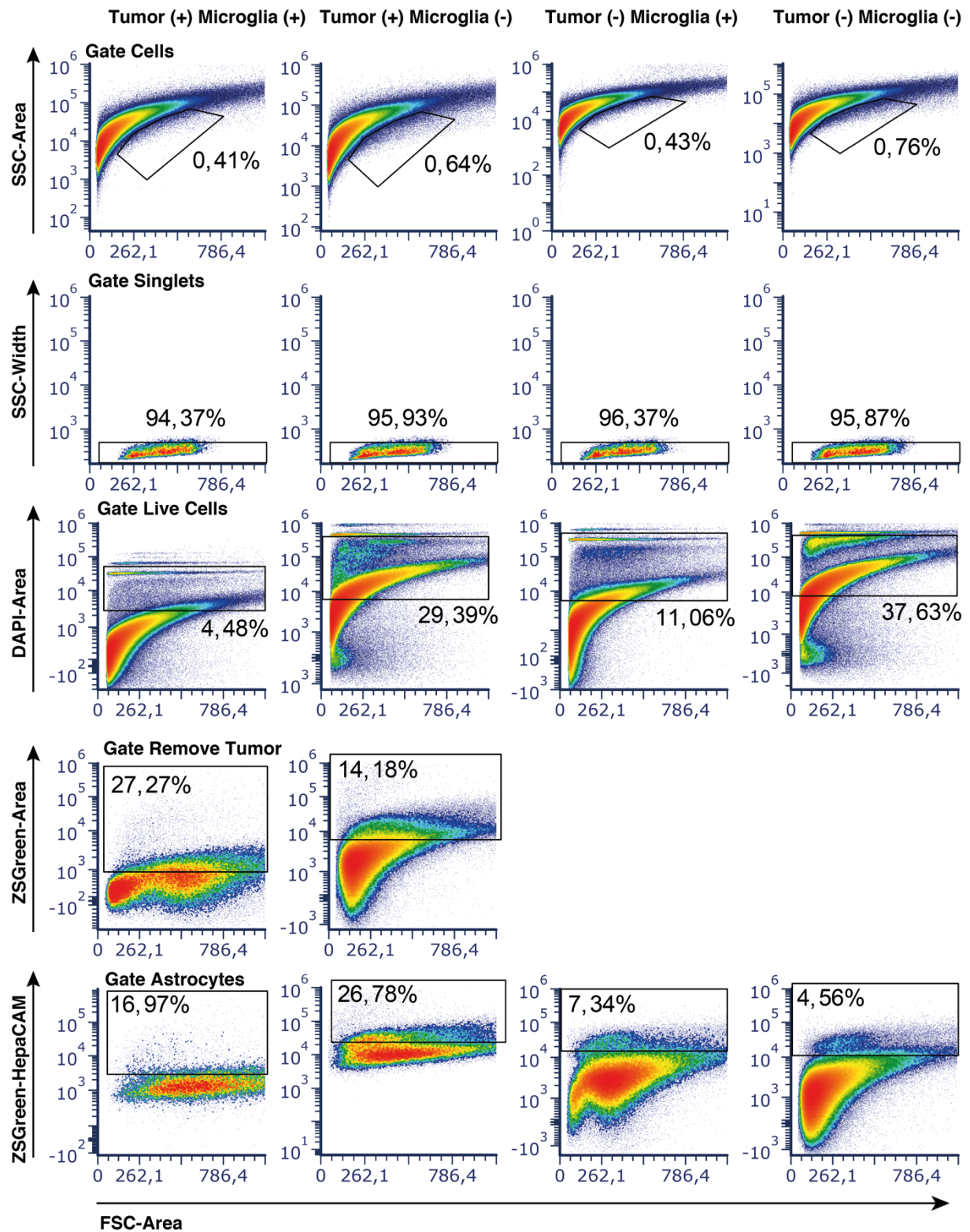
a) Western Blot of CD274, phosphorylated (STAT3-P) and total (STAT3-T) STAT3 of purified astrocytes from entry cortex of tumor patients and peritumoral tumor region. Actine is used for loading control **b)** Density plot of FCS area and HepaCAM area from peritumoral tumor region illustrates the gating of astrocytes. Detailed gating strategie is given in the **Supplementary Figure 8** **c)** Intensity histogram shows the increased amount of STAT3 phosphorylation in peritumoral astrocytes, quantified in the bar plot in **d)**. P-values were determined by two-tailed Student's t-test (d). Data is given as mean \pm standard deviation.



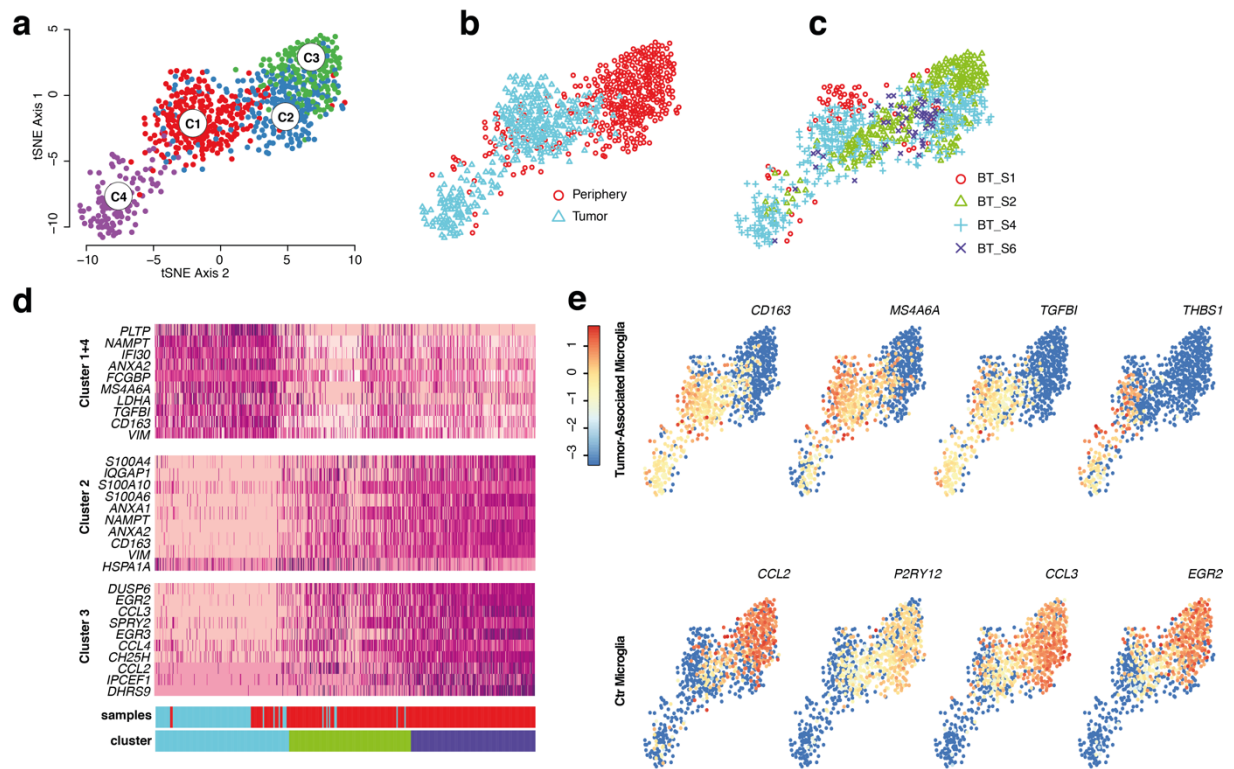
Supplementary Figure6: A detailed illustration is given to show the experimental time course in our novel slice model **a)** After the tumor injection, slices were either used as Microglia(+) or treated with Clodronate (3 days) in order to deplete microglia (Microglia(-) Slices).**b)** After tumor injection slices were incubated for 7 days with and without co-culture of an astrocyte cell line. **c)** After 10 days, astrocytes were purified and analyzed by various methods.



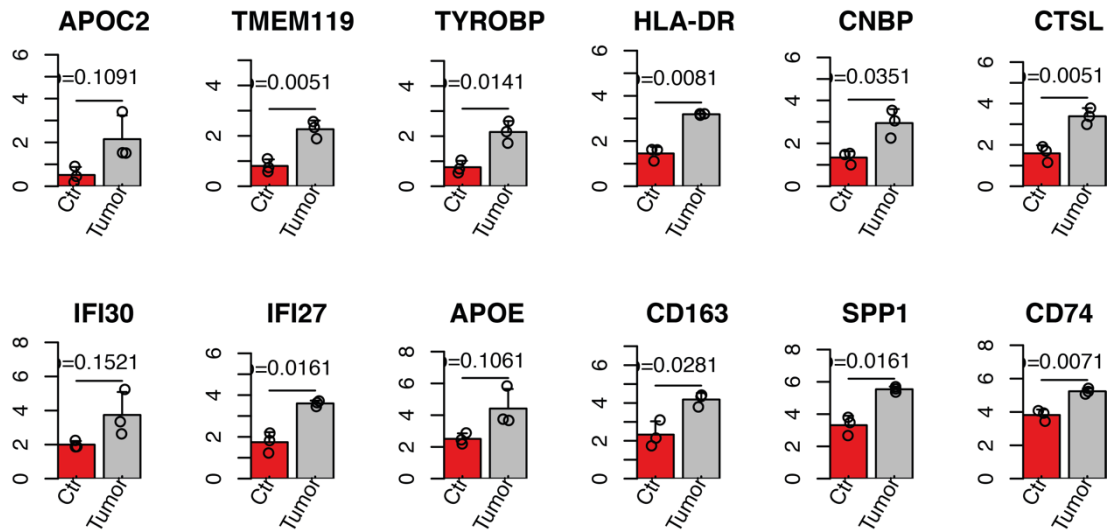
Supplementary Figure7: a) A heatmap of expression data from purified astrocytes of neocortical organotypic slices in four different conditions [Ctr: *Tumor(-) Microglia(+)*, with tumor injection: *Tumor(+)* *Microglia(+)*, without tumor and microglia depletion: *Tumor(-) Microglia(-)* and tumor injection in microglia depleted slices: *Tumor(+)* *Microglia(-)*] illustrates an unsupervised clustering by AutoPipe (CRAN: <https://cran.rproject.org/web/packages-/AutoPipe/>). The clustering revealed 3 different cluster by gap-statistics, cluster composition is given in the bars of the bottom. b) Gene Set Enrichment Analysis of the unique associated genes of each cluster (given by PAMR score), the bar plots illustrate the gene set enrichment for the top 5 pathways. c) Bar plots of 8 most differently regulated genes in ctr tumor associated astrocytes vs. astrocytes from microglia depletion. Expression values of the x-axis are normalized log2 transformed count data. P-values were determined by one-way ANOVA adjusted by Benjamini-Hochberger for multiple testing. Data is given as mean \pm standard deviation.



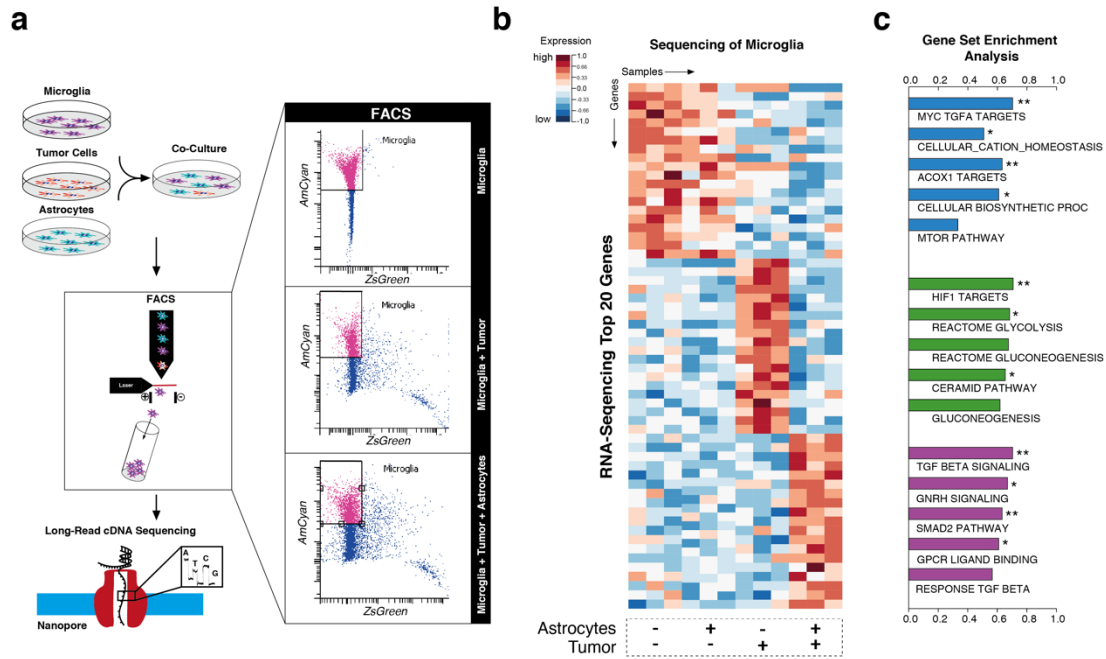
Supplementary Figure8: a) FACS density plot of gating in analysis of our slice model.



Supplementary Figure9: a) Analysis of single-cell RNA sequencing Data from Darmanis and colleagues. Microglia cells were isolated from the dataset. TSNE map of RaceID clustering revealed 4 microglia cluster with distinct transcriptional differences between tumor and infiltrating regions **b**) and patients **c**). Clustering of most differently expressed genes of the tumor associated genes was illustrated in **d**) and in colored TSNE maps in **e**).



Supplementary Figure 10: Bar plots of 12 most up-regulated genes from microglia in tumor injected slices vs. ctr. Expression values of the x-axis are normalized log₂ transformed count data. P-values were determined by two-tailed Student's t-test adjusted by Benjamini-Hochberger for multiple testing. Data is given as mean ± standard deviation.



Supplementary Figure 11 a) Illustration of the workflow and gating strategy. b) AutoPipe unsupervised cluster and heatmap of 20 signature genes of each experimental condition. The panel at the bottom indicates the presence of either microglia tumor cells or astrocytes. c) Gene set enrichment analysis (GSEA), highlighting an increased response to TGF β exclusively in the coexistence of astrocytes, tumor cells and microglia. * p-adjusted<0.01, ** p-adjusted<0.001, *** p-adjusted<0.0001.